

# Photon-induced self-trapping and entanglement of a bosonic Josephson junction inside an optical resonator

P. Rosson,<sup>1</sup> G. Mazarella,<sup>1</sup> G. Szirmai,<sup>2</sup> and L. Salasnich<sup>1,3</sup>

<sup>1</sup>*Dipartimento di Fisica e Astronomia “Galileo Galilei” and CNISM, Università di Padova, Via Marzolo 8, I-35131 Padova, Italy*

<sup>2</sup>*Institute for Solid State Physics and Optics, Wigner Research Centre for Physics, Hungarian Academy of Sciences, P.O. Box 49, H-1525 Budapest, Hungary*

<sup>3</sup>*CNR, INO, Via Nello Carrara 1, 50019 Sesto Fiorentino, Italy*

(Received 9 September 2015; revised manuscript received 2 November 2015; published 1 December 2015)

We study the influence of photons on the dynamics and the ground state of the atoms in a bosonic Josephson junction inside an optical resonator. The system is engineered in such a way that the atomic tunneling can be tuned by changing the number of photons in the cavity. In this setup the cavity photons are a means of control, which can be utilized both in inducing self-trapping solutions and in driving the crossover of the ground state from an atomic coherent state to a Schrödinger cat state. This is achieved, for suitable setup configurations, with interatomic interactions weaker than those required in the absence of a cavity. This is corroborated by the study of the entanglement entropy. In the presence of a laser, this quantum indicator attains its maximum value (which marks the formation of the catlike state and, at a semiclassical level, the onset of self-trapping) for attractions smaller than those of the bare junction.

DOI: [10.1103/PhysRevA.92.063604](https://doi.org/10.1103/PhysRevA.92.063604)

PACS number(s): 03.75.Lm, 05.70.Fh, 03.75.Gg, 03.67.—a

## I. INTRODUCTION

A Bose-Einstein condensate confined in a double-well potential mimics in many ways the coherent dynamics of a superconducting Josephson junction [1,2]. Therefore, it is often called a bosonic Josephson junction (BJJ), whose coherent dynamics can be described by the nonlinear equations of a nonrigid pendulum [2]. Furthermore, the investigation of the BJJ dynamics allows us to study the formation of macroscopic coherent states [2,3] and macroscopic Schrödinger cat states [4–10]. When the condensate is inside an optical resonator, the photon and atomic degrees of freedom are no longer independent [11]: There is a mutual backaction between the cavity and BJJ dynamics. The photon field acts as an optical potential on the atoms; at the same time, the atomic density serves as a refractive medium for the cavity photons. Note that the idea underlying this scheme is closely related to the models discussed, within the optical lattices context, in [12–14]. In an earlier paper it was shown how the constant photon field of a laser, tightly focused to the center of the junction barrier, influences the tunneling properties by effectively raising or lowering the barrier or ultimately allowing for a localized state inside the central well [15]. It was also investigated how the dynamical nature of a cavity field, focused similarly to the center of the barrier, alters the BJJ dynamics in the semiclassical level [16]. The purpose of this paper is to study how the photons influence the exact quantum dynamics and the ground state of the junction when the parameters of the system are chosen in such a way that the cavity field can be considered as fixed, i.e., in this bad cavity case the photon field is practically a laser field. The cavity photons alter the equations that describe the BJJ dynamics [16] and we investigate how they can induce self-trapping solutions. The study of the transition from the Josephson regime to the self-trapping regime in the semiclassical dynamics is complemented by the analysis of the ground state. The crossover from the atomic coherent state to the Schrödinger cat state can in fact be regarded as the quantum

counterpart to the semiclassical examination of the system. The ground state of the system is analyzed using three quantum indicators: the Fisher information, the coherence visibility, and the entanglement entropy. This last estimator proves to play a central role in understanding when the transition takes place.

## II. MODEL

Here we consider a hybrid system consisting of a BJJ and an optical cavity whose field is interacting with the atoms. The scheme is identical to that of Ref. [16] and is illustrated in Fig. 1. The BJJ in our system is made of an interacting Bose-Einstein condensate in a symmetric double-well potential. Its Hamiltonian in second-quantized form reads

$$\hat{H}_A = \int d^3\mathbf{r} \hat{\Psi}^\dagger(\mathbf{r}) \left[ -\frac{\hbar^2}{2m} \nabla^2 + V(\mathbf{r}) + \frac{g}{2} \hat{\Psi}^\dagger(\mathbf{r}) \hat{\Psi}(\mathbf{r}) \right] \hat{\Psi}(\mathbf{r}), \quad (1)$$

where  $\hat{\Psi}(\mathbf{r})$  annihilates an atom at position  $\mathbf{r} = (x, y, z)$ . Low-energy atom-atom scattering is characterized by  $g = 4\pi\hbar^2 a/m$ , where  $a$  is the  $s$ -wave scattering length and  $m$  is the mass of an atom. The confining potential is

$$V(\mathbf{r}) = V_{\text{DW}}(x) + \frac{1}{2}m\omega_H^2(y^2 + z^2), \quad (2)$$

where  $V_{\text{DW}}(x)$  is the double-well potential in the  $x$  direction, while we assume tight harmonic confinement in the transverse direction, with trap frequency  $\omega_H$ .

The optical cavity is a single-mode high- $Q$  Fabry-Pérot resonator whose axis is orthogonal to the double-well direction as depicted in Fig. 1. We choose the  $y$  direction for the cavity axis. The cavity has characteristic frequency  $\omega_C$ , it is pumped through one of its mirrors with a laser of frequency  $\omega_L$  and amplitude  $\eta$ , and it is operated in the TEM<sub>00</sub> mode. The mode function of the cavity is

$$f(\mathbf{r}) = \sqrt{\frac{2}{L}} \cos(ky) \frac{e^{-(x^2+z^2)/(2\sigma^2)}}{\pi^{1/2}\sigma}, \quad (3)$$

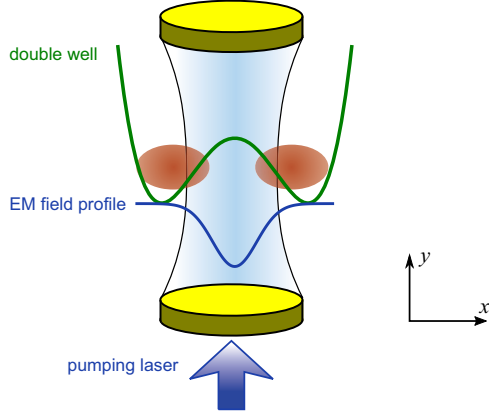


FIG. 1. (Color online) Illustration of the setup. The bosonic Josephson junction is created by magnetic or optical means along the  $x$  direction. A Fabry-Pérot cavity is placed around the junction with an axis orthogonal to the junction. The resonator is operated in the  $\text{TEM}_{00}$  mode.

where  $k = \omega_C/c$  is the wave number of the cavity mode,  $L$  is the distance between the mirrors, and  $\sigma$  is the width of the Gaussian profile in the  $(x, z)$  plane.

The cavity dynamics, in the frame rotating with a frequency  $\omega_L$  of the laser drive, is governed by the Hamiltonian

$$\hat{H}_C = -\hbar\Delta_C\hat{N}_L - i\hbar\eta(\hat{a} - \hat{a}^\dagger). \quad (4)$$

Here  $\Delta_C = \omega_L - \omega_C$  is the cavity detuning,  $\eta$  is the pumping strength of the driving laser,  $\hat{a}$  is the annihilation operator of a cavity photon, and  $\hat{N}_L = \hat{a}^\dagger\hat{a}$  is the photon number.

The condensate atoms have an electronic ground state and an excited state, with transition frequency  $\omega_A$ . We assume that the atomic detuning  $\Delta_A = \omega_L - \omega_A$  is large enough for the excited-state population to be negligible all the time and the atoms to behave as polarizable scalar particles. Therefore, their interaction with the cavity field is described by dispersive photon scattering [11], which shifts the cavity resonance frequency proportional to the atom number, and on the atomic degrees of freedom it creates an optical potential. This additional atom-light interaction term reads

$$\hat{H}_{AL} = \hbar U_0 \hat{a}^\dagger \hat{a} \int d^3\mathbf{r} f^2(\mathbf{r}) \hat{\Psi}^\dagger(\mathbf{r}) \hat{\Psi}(\mathbf{r}), \quad (5)$$

where the strength of the interaction is  $U_0 = \Omega_R^2/\Delta_A$ , with  $\Omega_R$  the single-photon Rabi frequency. As the cavity field is focused symmetrically to the center of the double-well barrier, the optical potential creates a symmetric light shift in the wells and lowers (raises) the height of the barrier for red- (blue-) detuned atoms.

When the double-well barrier is sufficiently high, the lowest-energy doublet is well separated from the rest of the spectrum. In this case the atomic dynamics can be constrained to the two-mode Fock space of the left and right valleys [2] and the atomic field operator can be approximated as

$$\hat{\Psi}(\mathbf{r}) = [w_1(x)\hat{b}_1 + w_2(x)\hat{b}_2] \frac{e^{-(y^2+z^2)/(2l_H^2)}}{\pi^{1/2}l_H}, \quad (6)$$

where  $\hat{b}_1$  and  $\hat{b}_2$  are the annihilation operators of a boson in the Wannier-like states  $w_1(x)$  and  $w_2(x)$ , centered around

the minima of the left and right valleys, respectively. The characteristic length of the strong harmonic confinement in the  $(y, z)$  plane is given by  $l_H = \sqrt{\hbar/m\omega_H}$ . In this limit, the Hamiltonian describing the BJJ dynamics is evaluated by inserting the field operator (6) into the atomic Hamiltonian (1),

$$\hat{H}_{\text{BJJ}} = \epsilon\hat{N} - J(\hat{b}_1^\dagger\hat{b}_2 + \hat{b}_2^\dagger\hat{b}_1) + \frac{U}{2}(\hat{b}_1^\dagger\hat{b}_1^\dagger\hat{b}_1\hat{b}_1 + \hat{b}_2^\dagger\hat{b}_2^\dagger\hat{b}_2\hat{b}_2). \quad (7)$$

The parameters  $\epsilon$ ,  $J > 0$ , and  $U$  are the on-site energy of a single well, the tunneling amplitude, and the on-site interaction energy, respectively. The values of these parameters are written in terms of overlap integrals of the Wannier functions [16].

Similarly, the atom-light interaction (5) is evaluated as

$$\hat{H}_I = \hat{N}_L [W_0\hat{N} + W_{12}(\hat{b}_1^\dagger\hat{b}_2 + \hat{b}_2^\dagger\hat{b}_1)]. \quad (8)$$

The term with  $W_0$  is the symmetric ac Stark shift, while the  $W_{12}$  term is the consequence of the lowering of the barrier. The latter can be understood as a cavity-assisted tunneling contribution. The values of the parameters  $W_0$  and  $W_{12}$  are also expressed as overlap integrals [16]. The full Hamiltonian of the system can be written as

$$\begin{aligned} \hat{H} &= \hat{H}_{\text{BJJ}} + \hat{H}_C + \hat{H}_I \\ &= (\epsilon + W_0\hat{N}_L)\hat{N} - (J - W_{12}\hat{N}_L)(\hat{b}_1^\dagger\hat{b}_2 + \hat{b}_2^\dagger\hat{b}_1) \\ &\quad + \frac{U}{2}(\hat{b}_1^\dagger\hat{b}_1^\dagger\hat{b}_1\hat{b}_1 + \hat{b}_2^\dagger\hat{b}_2^\dagger\hat{b}_2\hat{b}_2) - \hbar\Delta_C\hat{N}_L - i\hbar\eta(\hat{a} - \hat{a}^\dagger), \end{aligned} \quad (9)$$

A more detailed derivation of the Hamiltonian can be found in Ref. [16]. In this configuration,  $W_0$  and  $W_{12}$  can be either positive or negative since they are proportional to the atomic detuning  $\Delta_A$  [16]. If the atoms are red detuned, i.e.,  $\Delta_A < 0$ , both  $W_0, W_{12} < 0$ , while for blue detuning, i.e.,  $\Delta_A > 0$ , one has  $W_0, W_{12} > 0$ . The geometry of the system has a remarkable advantage: The cavity photons can influence the tunneling of the atoms between the two wells of the potential, as opposed to previous proposals of this type of system [17–19] that considered only the effect of the cavity photons on the on-site energies of the BJJ.

### III. SEMICLASSICAL APPROXIMATION

Let us assume that the system is in a fully coherent state  $\mathcal{S}$ , in which both the atoms in the right and left wells and the cavity photons are described with coherent states  $|\mathcal{S}\rangle = |\beta_1\rangle \otimes |\beta_2\rangle \otimes |\alpha\rangle$ , where  $\hat{b}_j|\beta_j\rangle = \beta_j|\beta_j\rangle$  and  $\hat{a}|\alpha\rangle = \alpha|\alpha\rangle$ . It is convenient to write the eigenvalues of the atomic coherent state as  $\beta_j = \sqrt{N_j}e^{i\theta_j}$ , where  $N_j$  is the average number of atoms in the  $j$ th well and  $\theta_j$  is the corresponding phase, and similarly  $\alpha = \xi e^{i\phi}$ , where  $N_L = \xi^2$  is the average number of photons in the cavity and  $\phi$  is the corresponding phase. The dynamics of the system can be described by a set of four ordinary differential equations for the fractional imbalance of the atomic population of the wells  $z = \frac{N_1 - N_2}{N}$ , the atomic relative phase  $\theta = \theta_2 - \theta_1$ , and the photon variables  $\xi$  and  $\phi$  [16]. The photon dynamics can be adiabatically eliminated when  $\delta_C = \Delta_C - N(W_0 + W_{12}\sqrt{1 - z^2}\cos\theta)/\hbar$  is orders of magnitude larger than  $\hbar^{-1}\nu = (J - W_{12}\xi^2)/\hbar^2$  [11]. When the

magnitude of the cavity detuning  $\Delta_C$  is much larger than that of  $NW_0/\hbar$  and  $NW_{12}/\hbar$  the system is described by

$$\dot{z} = -2\bar{v}\sqrt{1-z^2}\sin\theta, \quad (10a)$$

$$\dot{\theta} = \left( \bar{g} + \frac{2\bar{v}}{\sqrt{1-z^2}}\cos\theta \right) z, \quad (10b)$$

where  $\bar{v} = (J - W_{12}\xi^2)/\hbar = (J - W_{12}\eta^2/\delta_C^2)/\hbar$ . When these conditions are satisfied, the photon field amplitude  $\xi$  can be considered to be constant in time and  $\xi = \eta/|\Delta_C|$ . This set of equations is very similar to the Josephson equations for a bare Josephson junction. However here, because of the cavity photons, the tunneling amplitude  $J$  is replaced with the assisted tunneling amplitude  $\tilde{J} = J - W_{12}\xi^2$ . In the case of the bare BJJ the solutions to these equations can be divided into two classes. One is characterized by oscillations around  $z = 0$  and therefore the time average of the population imbalance is zero (Josephson regime). The second class of solutions is characterized by an average imbalance in the population of the wells (self-trapping regime). However, in our system, the cavity photons can be used to induce self-trapping solutions for initial conditions and parameters that would not allow them in the bare junction. When  $U > 0$  and  $\tilde{J} > 0$ , the self-trapping occurs when [2]

$$\frac{\Lambda}{2}z^2(0) - \sqrt{1-z^2(0)}\cos\theta(0) > 1, \quad (11)$$

where  $\Lambda = UN/2\tilde{J}$  and  $z(0)$  and  $\theta(0)$  are the initial conditions to the equations. Since  $\Lambda$  depends on the number of cavity

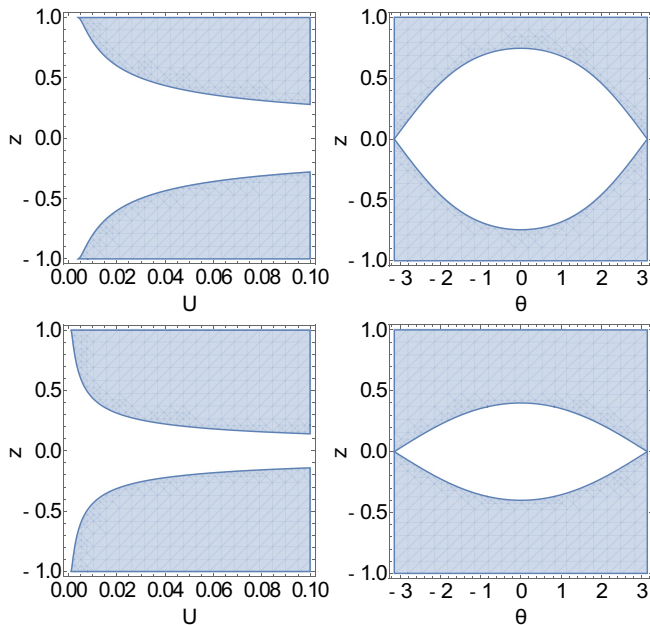


FIG. 2. (Color online) The highlighted area in each panel shows the values of  $z$ ,  $U$ , and  $\theta$  that allow self-trapping for a fixed  $\theta = 0$  (left-hand column) and a fixed  $U = 12J/N$  (right-hand column). The difference between the two rows is the number of photons in the cavity. In the top row  $\xi^2 = 0$  and  $\tilde{J} = J$  and in the bottom  $\xi^2 = 25$  and  $\tilde{J} = 0.25J$ . It is clear that, because of the cavity photons, the highlighted area gets wider and therefore the appearance of the self-trapping is assisted. The other parameters are  $N = 1000$  and  $NW_{12} = 30J$ . Here  $U$  is written in units of  $J$ .

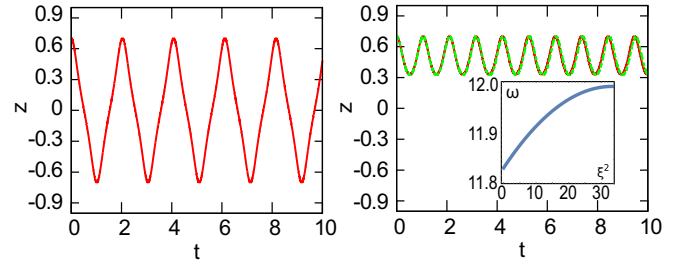


FIG. 3. (Color online) Time evolution of the variable  $z$ . Time is measured in units of  $\hbar/J$ . Shown on the left is the bare junction in the absence of the cavity and on the right the junction inside the cavity. The solid lines represent the numerical solution of the system (10), where the photon variables are constant. The dashed line represents the solution of the system where the photon dynamics has not been adiabatically eliminated. When there are no photons, the system is in the Josephson regime, while when the photon number is increased the system is in the self-trapped regime. The parameters for the second panel are  $\hbar\Delta_C = 300J$ ,  $W_0N = 4J$ ,  $W_{12}N = 3J$ ,  $UN = 12J$ ,  $N = 1000$ , and  $\hbar\eta = 3000J$ . The initial conditions are  $(z, \theta) = (0.7, 0)$  (left) and  $(z, \theta, \xi, \phi) = (0.7, 0, 10.17, \pi/2)$  (right). The inset represents the frequency  $\omega$  of the small oscillations of  $z$  written as a function of the number of cavity photons  $\xi^2$ ;  $\omega$  is written in units of  $J/\hbar$ . The range of  $\xi^2$  is given by the condition for the system to show small oscillations. The other relevant parameters for the inset are  $N = 1000$ ,  $UN = 0.012J$ , and  $W_{12}N = 0.03J$ .

photons  $\xi^2$ , in our system we have one more relevant parameter that allows us to switch between different regimes.

By comparing the panels in Fig. 2, it can be clearly seen what the effect of changing the number of photons is when  $W_{12} > 0$ . In particular we notice how increasing the number of photons widens the area that allows self-trapping solutions.

The photon-induced change of regime can be clearly seen in Fig. 3. The left panel shows the time evolution of  $z$  in the Josephson regime, in the absence of photons. The right panel shows the time evolution when the cavity photons are present in the system: It can be clearly seen that the photons induce oscillations around a nonzero average value of  $z$ . The cavity photons can therefore be used as a means of inducing self-trapped solutions that would not otherwise occur in the absence of the cavity.

#### IV. EXACT DIAGONALIZATION

We now want to show how the cavity photons influence the ground state of the system. In order to do this, we describe the photons with a coherent state  $|\alpha\rangle$ , but we describe the atoms in the wells in a purely quantum way. To this end we use Fock states as basis vectors in the atomic Hilbert space. Furthermore, we assume that the photon field relaxes quickly and this allows us to consider the photon coherent state to be a parameter on which the atomic ground state depends. The ground state of the atomic field for a given photon field coherent state  $|\alpha\rangle$  can be written as  $|\text{g.s.}\rangle_\alpha = \sum_n c_n(\alpha)|n\rangle$ , where  $|n\rangle = |N-n, n\rangle$  is an element of the Fock basis  $\{|n\rangle, n = 0, 1, \dots, N\}$  and  $N$  is the total number of atoms. The element of the Fock basis  $|n\rangle$  describes the state in which  $n$  atoms are in the

right well and  $N - n$  in the left well. The coefficients  $c_n(\alpha)$  clearly depend on the photon field. So the ground state of the system can be written as  $|\text{g.s.}\rangle = |\alpha\rangle \otimes |\text{g.s.}\rangle_\alpha$ , which is the tensor product of the coherent state of the photon field and of the atomic ground state for that field strength. In order to calculate the ground-state coefficients  $c_n(\alpha)$  the matrix elements of the Hamiltonian that needs to be diagonalized are

$$\begin{aligned} H_{m,n}(\alpha) = & -(J - W_{12}|\alpha|^2)(\sqrt{N - m}\sqrt{n}\delta_{m,n-1} \\ & + \sqrt{N - n}\sqrt{m}\delta_{m,n+1}) + \frac{U}{2}[(N - n)(N - n - 1) \\ & + n(n - 1)]\delta_{m,n}. \end{aligned} \quad (12)$$

If we assume that the photon field relaxes very fast, then  $i\hbar \frac{d}{dt}\alpha = 0$  leads to a relation between  $\alpha$  and the ground-state coefficients  $c_n(\alpha)$  that needs to be satisfied in order for the computation of the ground state to be consistent. This makes the amplitude of the photon field  $|\alpha\rangle$  dependent on the parameters that appear in the Hamiltonian and on the coefficients  $c_n(\alpha)$  as well. The analysis of the ground state can however be simplified when  $|\Delta_C| \gg |W_0|N/\hbar$  and  $|\Delta_C| \gg |W_{12}|N/\hbar$ . When such conditions are satisfied  $\alpha$  depends weakly on the coefficients  $c_n(\alpha)$ . Therefore, for any starting number of photons  $|\alpha|^2$  the above procedure gives as a result the starting  $|\alpha|^2$ . The number of photons in the system can thus be modified by changing the values of  $\eta$  and  $\Delta_C$ . Under this approximation we only need to study how the ground state of the Hamiltonian with the assisted tunneling is influenced by the presence of the photons. In the absence of the cavity, and thus  $|\alpha|^2 = 0$ , the ground state of the BJJ can show three limit behaviors depending on the value of the ratio  $U/J$  [20]. When  $U/J = 0$  the ground state is an atomic coherent state, where the distribution of the  $|c_n(\alpha)|^2$  has a Gaussian profile. For large values  $|U/J|$  the ground state can be found in two configurations, depending on the sign of  $U/J$ . When  $U/J > 0$  the ground state is a separable Fock state, where half of the atoms are in the right well and half in the left one. When  $U/J < 0$  the ground state is a Schrödinger cat state, which is the linear combination of the states with all particles in the left or in the right well. Changing the interaction strength  $U/J$  leads to a continuous transitions between these three kinds of states.

The correlation properties of the ground state can be analyzed by using the Fisher information  $F$  [21,22] and the coherence visibility  $\alpha_v$  [23]. The definition for these two estimators can be found in [20]. In particular,  $F$  gives the width of the distribution of  $|c_n(\alpha)|^2$  and  $\alpha_v$  characterizes the degree of coherence between the two wells. We are interested in characterizing also the genuine quantum correlations between the atoms in two wells pertaining to the ground state. Here we focus on the atom part only and address this issue from the bipartition perspective with the two wells playing the role of the two partitions. Following the same path as in [20,24], we thus calculate the entanglement entropy  $S$  [25] that results in  $S = -\sum_{n=0}^N |c_n(\alpha)|^2 \log_2 |c_n(\alpha)|^2$ . Remarkably,  $S$ , plotted as a function of  $U$ , shows a maximum at the onset of the transition to the Schrödinger-catlike-state regime in which the distribution of the  $|c_n(\alpha)|^2$  begins to exhibit a valley. The Hamiltonian

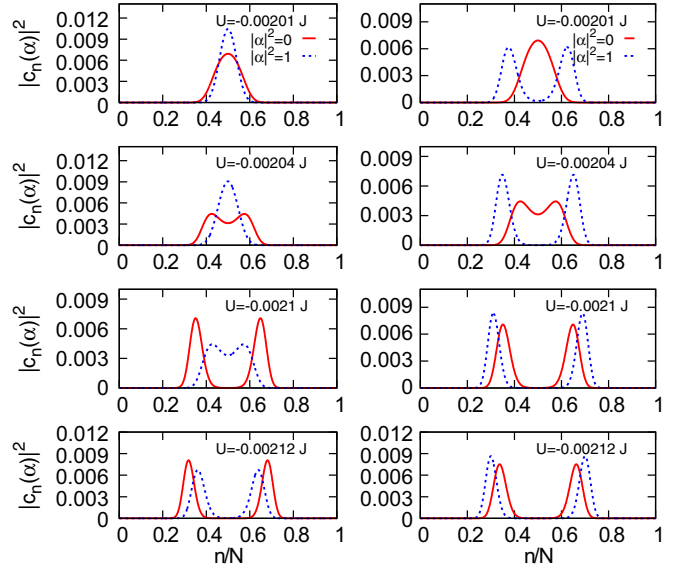


FIG. 4. (Color online) Coefficients  $|c_n(\alpha)|^2$  of the ground state as a function of  $n/N$  for  $N = 1000$ . In the left-hand column  $W_{12} = -0.03J$  and in the right-hand column  $W_{12} = 0.03J$ . The on-site interaction is negative  $U < 0$ . The solid line represents the system in the absence of cavity photons  $|\alpha|^2 = 0$ , while the dashed line represents the system when  $|\alpha|^2 = 1$ . The effect of the cavity photons in the left-hand column is to increase the coherence of the ground state for a given negative on-site interaction  $U$  and thus delay the transition to the regime in which a valley appears in the middle of the distribution of the coefficients  $|c_n(\alpha)|^2$ . The effect of the cavity photons in the right-hand column is the opposite. The coherence of the ground state decreases for a given negative on-site interaction  $U$  and thus the photons assist the transition to the regime in which a valley appears in the middle of the distribution of the coefficients  $|c_n(\alpha)|^2$ . In both cases the ground state is shown for four values of  $U$ . The coefficients  $|c_n(\alpha)|^2$  are adimensional and normalized so that  $\sum_{n=0}^N |c_n(\alpha)|^2 = 1$ ;  $n/N$  is adimensional.

we need to diagonalize in Eq. (12) differs from the Hamiltonian of a bosonic Josephson junction only for the value of the tunneling amplitude, which we will call  $\tilde{J} = J - W_{12}|\alpha|^2$ . The magnitude and sign of  $\tilde{J}$  depend on both  $W_{12}$  and the photon number  $|\alpha|^2$ .

When  $W_{12} < 0$  the assisted tunneling amplitude  $\tilde{J}$  is always positive and its magnitude gets larger as the number of photons in the system  $|\alpha|^2$  increases. Let us choose  $W_{12} = -0.03J$  and plot together the ground states for various values of  $U$  for  $|\alpha|^2 = 1$  and therefore  $\tilde{J} = 1.03J$ . We always plot the ground state of the bare junction, with  $|\alpha|^2 = 0$ , to use as a reference. In the left-hand columns Figs. 4 and 5 we can see what happens when the on-site interaction  $U$  is negative. When the interaction is positive, the effect of the photons is still to delay the transition to the separable Fock state.

When  $W_{12} > 0$  the assisted tunneling amplitude  $\tilde{J}$  gets smaller when increasing the number of photons in the cavity. This can lead to two main consequences. On the one hand, if the number of photons is sufficiently small,  $\tilde{J}$  maintains its positive sign but its magnitude gets smaller and  $0 < \tilde{J}/J < 1$ . On the other hand, if the number of photons is large enough the assisted tunneling can become negative  $\tilde{J}/J < 0$ . When

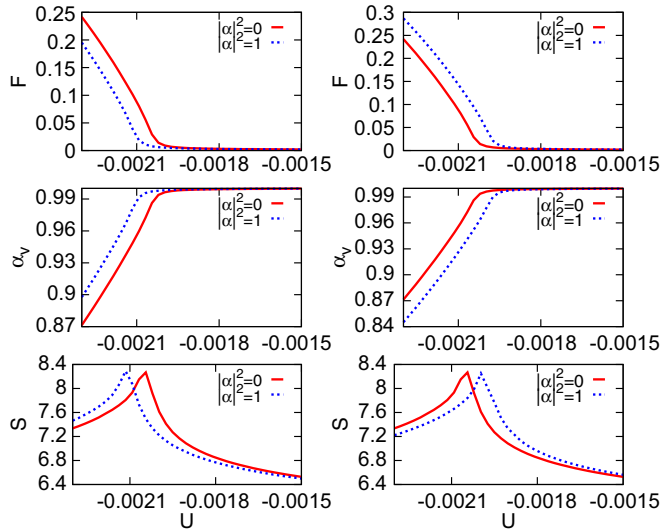


FIG. 5. (Color online) Fisher information  $F$ , coherence visibility  $\alpha_v$ , and entanglement entropy  $S$  plotted as a function of the on-site interaction  $U$ , which is written in units of  $J$ , for  $N = 1000$ . In the left-hand column  $W_{12} = -0.03J$  and in the right-hand column  $W_{12} = 0.03J$ . The solid line represents the system when  $|\alpha|^2 = 0$ , while the dashed line represents the system when  $|\alpha|^2 = 1$ . The on-site interaction is attractive  $U < 0$ . The plots of the quantum indicators complement those of Fig. 4. In the presence of photons  $F$  is smaller when  $W_{12} < 0$  and larger when  $W_{12} > 0$ , compared to the solid line, since  $F$  is related to the distribution width of the  $c_n(\alpha)$ . Here  $\alpha_v$  is larger for  $W_{12} < 0$  and smaller for  $W_{12} > 0$  compared to the solid line as the photons increase and decrease the coherence, respectively. Further,  $S$ , whose maximum represents the value of  $U$  at which the distribution of the  $|c_n(\alpha)|^2$  starts to show a valley [20], appears for a larger  $|U|$  for  $W_{12} < 0$  and for a smaller  $|U|$  for  $W_{12} > 0$ . The values of  $F$ ,  $\alpha_v$ , and  $S$  are dimensionless.

$0 < \tilde{J}/J < 1$  we can plot the ground states of the system for different values of negative  $U$  and for  $|\alpha|^2 = 1$ , and therefore  $\tilde{J} = 0.97J$ . We can see from the right-hand columns in Figs. 4 and 5 that the effect of the photons in this case is opposite to the effect when  $W_{12}$  is negative. When the interaction is positive, the effect of the photons is still to assist the transition to the separable Fock state. It is worth mentioning that this result is actually more interesting than the sole rescaling of the ratio  $U/J$ . Focusing our attention on the attractive on-site interaction and on the emergence of the Schrödinger-catlike-state regime, we can notice a fundamental difference. For a fixed number of atoms in the system, in the bare Josephson junction, the transition to the Schrödinger-catlike-state regime happens for a definite value of  $U/J$ . However, in the complete system, with a positive  $W_{12}$ , by fine-tuning the number of cavity photons, the transition to the Schrödinger-catlike-state regime can happen for a given magnitude of negative  $U$ , without changing the number of atoms. This means that the photons in the system act as a new knob through which the transition between different regimes can be manipulated. The change of the sign of  $\tilde{J}$  is significant when analyzing the Hamiltonian of the system. In the case of the bare Josephson junction  $J$  can always be taken to be positive. However, by numerically calculating the ground state of the system we

found that the sign of  $\tilde{J}$  bears no relevance to the coefficients  $|c_n(\alpha)|^2$  and to the value of the quantum indicators. Therefore, choosing values of  $|\alpha|^2$  such that the values of the assisted tunneling amplitude  $\tilde{J}$  are the same as the ones we have just studied, but with opposite signs, leads to the same results. It is interesting to note this analogy between the case with positive  $\tilde{J}$  and negative  $\tilde{J}$ . One would at first think that, since the relevant parameter in the analysis is the ratio  $U/\tilde{J}$ , when  $\tilde{J}$  is negative, the same results could be obtained by changing the sign of  $U$  as well; however this is not the case.

## V. SUMMARY

We have shown that the cavity photons can be used to induce self-trapping solutions in the dynamics of the Josephson junction. Moreover, we have described how the transition from the atomic coherent state to a Schrödinger cat state can be delayed or expedited, depending on the photon-assisted tunneling amplitude. This analysis is the foundation of the quantum study of this system. Possible extensions of this work could be the study of the ground state when the  $|\Delta_C| \gg |W_0|N/\hbar$  and  $|\Delta_C| \gg |W_{12}|N/\hbar$  conditions no longer hold. This would lead to the same ground states we have already found, but the photon number of the cavity would depend on the other parameters of the system. Moreover, one could try to better understand the transition between the atomic coherent state and the Schrödinger cat state, by computing the relevant critical indices for  $F$  and  $\alpha_v$ .

The setup considered here can be implemented directly due to the current feasibility of trapping ultracold bosons in double-well potentials [26–28] and to fabricate high-finesse optical cavities supporting quantum degenerate bosonic clouds [29–31]. The experiment deriving from the suitable combination of these two parts would provide a powerful tool for observing the Josephson–self-trapping crossover, an issue addressed with bare BJJs [26] and creating entangled states of matter. In this context, experimentalists could have the concrete possibility to receive feedback on the shift of the crossover above by using the number of cavity photons as a knob. The setup considered in Ref. [30] is extremely appealing, where the Fabry-Pérot cavity is assembled on top of an atom chip, where wires suitable for the double-well potential can be easily placed too. On such a device one has to fine-tune experimental parameters that mainly consist in the proper matching of the double-well dimensions (a barrier width of a few microns) with those of the waist of the cavity (also in the range of a few microns).

## ACKNOWLEDGMENTS

The authors acknowledge Italian Ministry of Education, University and Research for partial support (PRIN Project No. 2010LLKJBX “Collective Quantum Phenomena: From Strongly-Correlated Systems to Quantum Simulators”). G.S. also acknowledges support from the Hungarian Scientific Research Fund (Grant No. PD104652) and the János Bolyai Scholarship.

- [1] B. D. Josephson, *Phys. Lett.* **1**, 251 (1962).
- [2] S. Raghavan, A. Smerzi, S. Fantoni, and S. R. Shenoy, *Phys. Rev. A* **59**, 620 (1999).
- [3] L. Pitaevskii and S. Stringari, *Phys. Rev. Lett.* **83**, 4237 (1999); **87**, 180402 (2001).
- [4] J. I. Cirac, M. Lewenstein, K. Molmer, and P. Zoller, *Phys. Rev. A* **57**, 1208 (1998).
- [5] B. Juliá-Díaz, D. Dagnino, M. Lewenstein, J. Martorell, and A. Polls, *Phys. Rev. A* **81**, 023615 (2010).
- [6] B. Juliá-Díaz, J. Martorell, and A. Polls, *Phys. Rev. A* **81**, 063625 (2010).
- [7] Y. P. Huang and M. G. Moore, *Phys. Rev. A* **73**, 023606 (2006).
- [8] D. W. Hallwood, T. Ernst, and J. Brand, *Phys. Rev. A* **82**, 063623 (2010).
- [9] L. D. Carr, D. R. Dounas-Frazer, and M. A. Garcia-March, *Europhys. Lett.* **90**, 10005 (2010).
- [10] M. A. Garcia-March, D. R. Dounas-Frazer, and Lincoln D. Carr, *Front. Phys.* **7**, 131 (2012).
- [11] H. Ritsch, P. Domokos, F. Brennecke, and T. Esslinger, *Rev. Mod. Phys.* **85**, 553 (2013).
- [12] C. Maschler, H. Ritsch, A. Vukics, and P. Domokos, *Opt. Commun.* **273**, 446 (2007).
- [13] C. Maschler, I. B. Mekhov, and H. Ritsch, *Eur. Phys. J. D* **46**, 545 (2013).
- [14] S. F. Caballero-Benitez and I. B. Mekhov, [arXiv:1504.06581](https://arxiv.org/abs/1504.06581).
- [15] G. Szirmai, G. Mazzarella, and L. Salasnich, *Phys. Rev. A* **90**, 013607 (2014).
- [16] G. Szirmai, G. Mazzarella, and L. Salasnich, *Phys. Rev. A* **91**, 023601 (2015).
- [17] J. F. Corney and G. J. Milburn, *Phys. Rev. A* **58**, 2399 (1998).
- [18] J. M. Zhang, W. M. Liu, and D. L. Zhou, *Phys. Rev. A* **77**, 033620 (2008).
- [19] M. Zuppardo, J. P. Santos, G. De Chiara, M. Paternostro, F. L. Semiao, and G. M. Palma, *Phys. Rev. A* **91**, 033631 (2015).
- [20] G. Mazzarella, L. Salasnich, A. Parola, and F. Toigo, *Phys. Rev. A* **83**, 053607 (2011).
- [21] L. Pezzé and A. Smerzi, *Phys. Rev. Lett.* **102**, 100401 (2009).
- [22] B. Gertjerenken, S. Arlinghaus, N. Teichmann, and C. Weiss, *Phys. Rev. A* **82**, 023620 (2010).
- [23] G. Ferrini, A. Minguzzi, and F. W. J. Hekking, *Phys. Rev. A* **78**, 023606(R) (2008).
- [24] M. Galante, G. Mazzarella, and L. Salasnich, *Rom. Rep. Phys.* **67**, 273 (2015).
- [25] C. H. Bennett, H. J. Bernstein, S. Popescu, and B. Schumacher, *Phys. Rev. A* **53**, 2046 (1996).
- [26] M. Albiez, R. Gati, J. Fölling, S. Hunsmann, M. Cristiani, and M. K. Oberthaler, *Phys. Rev. Lett.* **95**, 010402 (2005).
- [27] T. Schumm, S. Hofferberth, L. M. Andersson, S. Wildermuth, S. Groth, I. Bar-Joseph, J. Schmiedmayer, and P. Krüger, *Nat. Phys.* **1**, 57 (2005).
- [28] S. Levy, E. Lahoud, I. Shomroni, and J. Steinhauer, *Nature (London)* **449**, 579 (2007).
- [29] F. Brennecke, T. Donner, S. Ritter, T. Bourdel, M. Köhl, and T. Esslinger, *Nature (London)* **450**, 268 (2007).
- [30] Y. Colombe, T. Steinmetz, G. Dubois, F. Linke, D. Hunger, and J. Reichel, *Nature (London)* **450**, 272 (2007).
- [31] K. W. Murch, K. L. Moore, S. Gupta, and D. M. Stamper-Kurn, *Nat. Phys.* **4**, 561 (2008).